ELSEVIER

Catalysis Today 54 (1999) 507–519

CATALYSIS TODAY

www.elsevier.com/locate/cattod

Effect of the support upon the behavior of Cu in NO decomposition exemplified on Cu-ZSM-5 containing Zr

V.I. Pârvulescu [a], M.A. Centeno[b,1], O. Dupont [b], R. Bârjega [c], R. Ganea [c], B. Delmon [b,*], P. Grange [b]

[a] *University of Bucharest Department of Chemical Technology and Catalysis, B-dul Republicii 13, Bucharest, 70346, Romania*
[b] *Université Catholique de Louvain, Unité de Catalyse et Chimie des Matériaux Divisés Place Croix du Sud 2/17, 1348 Louvain-la-Neuve, Belgium*
[c] *ZECASIN Bucharest, Splaiul Independentei 202, Bucharest 77208, Romania*

Abstract

ZSM-5 containing Zr in the lattice was prepared following the procedure for ZSM-5 using $ZrCl_4$ as zirconium precursor. Zr was substituted for Si in the ZSM-5 lattice and then this zeolite was loaded with Cu. Loading these catalysts with Cu was carried out following Iwamoto's procedure. An increase in Zr results in a decrease in Cu loading, although the exchange solutions were the same. The increased Zr loading and, hence, decreased Cu loading resulted in a decreased NO decomposition activity relative to the Zr-free ZSM-5 loaded with Cu. NO conversions, obtained on Cu-ZSM-5 zeolites in which zirconium replaced Si, were below 40%, which is about 30% lower than those recorded on Cu-exchanged pure zeolites. The amount of NO_2 detected in the reaction products proved that, for total conversions lower than 20%, the reaction of NO takes place almost exclusively without decomposition to N_2 and O_2. The catalysts were characterized by DRIFTS and NO-DRIFTS, Raman spectroscopy, O_2 — TPD and XPS. The OH region observed in DRIFTS changed with an increase in Zr loading and, hence, Cu(II)–O–Cu(I) species cannot be formed. This may play a role in the decreased activity. Raman spectra showed that increased Zr also results in increased CuO which may lead to the decreased activity. Although the exposure of the samples with high Zr content to NO results in the apparent redispersion of CuO to isolated sites within the ZSM-5, the Cu moves to locations which are inactive and/or inaccessible to NO and, hence, the activity does not increase even though the Cu is dispersed. The formation of NO_2 follows the mechanism proposed by Shelef.

Keywords: Cu-ZSM-5; ZSM-5 containing Zr; NO-DRIFTS; Raman spectroscopy; O_2-TPD; XPS

1. Introduction

Since Iwamoto [1–3] reported high conversions in NO decomposition over Cu-ZSM-5, this has become one of the most investigated catalytic reactions. Almost all the factors that could influence the activity and stability of the catalysts were investigated and, quite logically, this included the nature and the characteristics of the support. However, in spite of the tremendous effort that has been done and the large amount

* Corresponding author. Tel.: +32-10-473591; fax: +32-10-473649
E-mail addresses: parvulescu@hotmail.com (V.I. Pârvulescu), delmon@cata.ucl.ac.be (B. Delmon), grange@cata.ucl.ac.be (P. Grange)

[1] On leave from Departamento de Quimica Inorganica e Instituto de Ciencia de Materiales de Sevilla, Centro de Investigaciones Cientificas Isla de la Cartuja, Universidad de Sevilla-CSIC, Sevilla, Spain.

0920-5861/99/$ – see front matter
PII: S0920-5861(99)00213-8

of evidence obtained, two questions have not yet been answered: why do only Cu and ZSM-5 allow a better conversion in NO decomposition?

Comparative studies performed by Iwamoto et al. [3,4] using various zeolites: faujasite, Y, mordenite or ZSM-5, and other supports, such as Al_2O_3 or SiO_2-Al_2O_3 indicated that the superiority of the ZSM-5 support was evident when comparing materials with the same copper content or, in the case of zeolites, for the same percentage of copper exchanged. Irrespective of the reaction conditions, the order was always the same, namely ZSM-5 $\gg$ Y $\cong$ mordenite $\gg$ faujasite. Moreover, the modification of the Si/Al ratio in ZSM-5 also resulted in a change in activity. Iwamoto et al. [4] reported that an Si/Al ratio of 40–100 corresponds to the highest activity. Li and Hall [5] and Moretti [6] found a decrease in the activity per copper atom when the Si/Al ratio ranged between 12 and 27. Other experiments made by Pârvulescu et al. [7] using over-exchanged Cu-ZSM-5 with Si/Al ratios between 15 and 60 indicated that an increase of the Si/Al ratio up to 25 led to an increase in the conversion, and the activity started to decrease at ratios >30. XPS studies of all these catalysts suggested a surprising redispersion of the copper-containing species at the surface and/or a migration to the inside of the zeolite. In this way, part of Cu moves to locations which are inactive and/or inaccessible to NO.

Several explanations have been proposed for this behavior. Centi and Perathoner [8] consider that two factors make the MFI structure of ZSM-5 more adequate than the other structures investigated: one geometrical and one electronic. For the first one, these authors speculate that, in all the other zeolites, part of the copper is implanted in hidden positions where the shielding effects of the lattice oxygen prevent or limit the possibility of interaction with the reactant molecules. In addition, the small pore diameter of ZSM-5 prevents the formation of large Cu aggregates such as in other oxide supports. The second effect is related to the covalency of the bond between the metal and the zeolite lattice, this decreasing in the order MFI > mordenite > faujasite. Because of this, the local charge 'sensed' by molecules coordinating the Cu ions differs considerably from one zeolite to another. In addition, Wichterlova et al., [9–11] have shown that four typical Cu sites exist in these zeolites because of the different distribution of Al, and mainly of 'Al pairs'.

The consequence is that the structure of the MFI zeolites offers a good environment for the formation of dispersed Cu active species, and the charge localized on these species can, in principle, be 'tuned' by modifying the charge associated to the exchangeable zeolite sites. In this context, one of the solutions proposed by Centi and Perathoner [8] for increasing the catalyst performance was to substitute the species constituting the zeolite framework with others. Replacing one element with another in the synthesis of the zeolite materials is restricted by the atomic ratio of the elements. Therefore, few combinations can be envisaged. Centi and Perathoner [8] reported that replacing Al with B gives a positive effect and they proposed this way as a possibility to improve the behavior of these catalysts. In order to verify such a hypothesis and possibly to identify some effects due to the support upon the catalytic behavior of Cu in NO decomposition, we worked with Cu-ZSM-5 in which some silicon was progressively replaced by Zr.

2. Experimental

ZSM-5 containing Zr was prepared following a procedure well known in MFI, using $ZrCl_4$as zirconium precursor [12]. A series of zeolites was prepared starting from an SiO_2/Al_2O_3 molar ratio of 15 and different ZrO_2/Al_2O_3 ratios, namely: 0, 0.5, 1.0, 1.5 and 2.0, respectively. The MFI structure was verified using XRD by recording the patterns of the samples in a step-scanning mode (step 0.02°) in the region of interest for MFI, namely $26 \leq 2\theta \leq 29^\circ$ (Fig. 1). The Zr-containing samples showed a tendency to adopt an orthorhombic symmetry as a sign of the presence of Zr^{4+} in the zeolite framework. The presence of the framework Zr^{4+} is detected from the evolution of the 313 and 313 planes [13,14]. An increase of the unit cell volume was also detected. Copper exchanged zeolites were prepared from copper (II) acetate monohydrate (purity > 98%) using a one-step exchange procedure [15]. According to this procedure, $15\,g\,l^{-1}$ of the parent H-ZSM-5 was suspended in 300 ml distilled water. The suspension was sonicated for 30 min, then 10^{-2} mol l^{-1}copper acetate was added. An exception is the sample Z-0-220, for which the

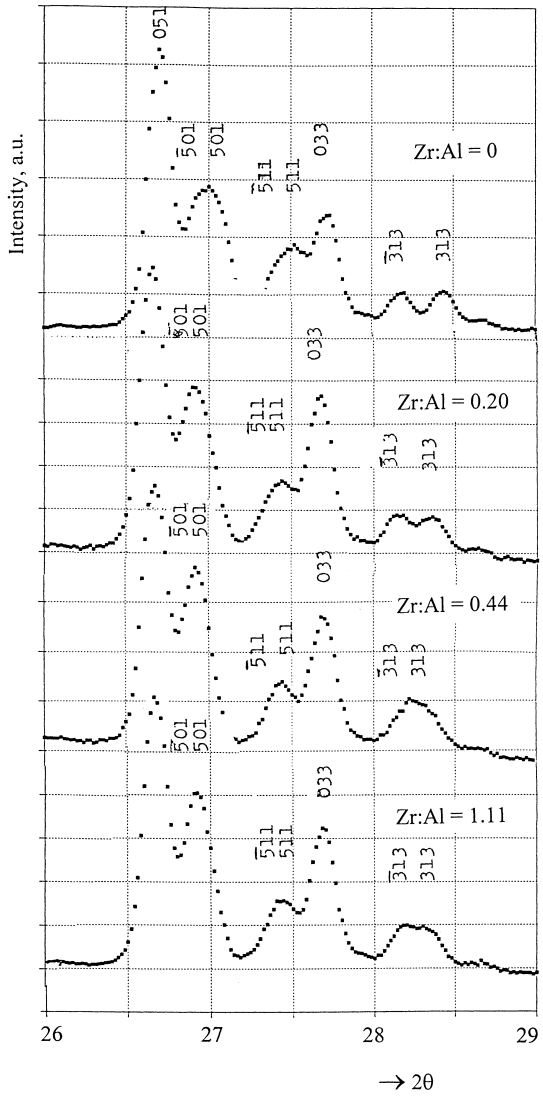

Fig. 1. XRD pattern of ZSM-5 containing Zr compared with pure ZSM-5 in the range $26<2\theta<29^{\circ}$.

amount of copper acetate added to the suspension was 8.5×10^{-3} mol l^{-1}. After stirring for 24 h, the pH was raised to neutrality with ammonia and the suspension stirred for 1.5 h. The sample was then centrifuged and redispersed in distilled water until the conductivity of the washing water was below 7 mS cm^{-1}. The solid was then dried overnight under vacuum, at room temperature, prior to pre-treatment. Elemental analysis of Si, Al, Zr, and Cu was performed by atomic emission spectroscopy with inductively coupled plasma atomization (ICP-AES) after drying of the samples overnight at 373 K (Table 1). ICP-AES analysis of the resulting samples corresponded to a (Si + Zr)/Al atomic ratio of ca. 30 and ZrO_2/Al_2O_3 ratios ranging from 0.01 to 0.89. An important decrease was observed in the Cu exchange degree when the Zr content in the zeolites increased, namely from over-exchanged zeolites (220 and 241% Cu exchange) to less-exchanged ones (85% Cu exchange) (Table 1). The basis for the calculation of the exchanged Cu was 1Cu/2Al = 100%. Before the catalytic tests the zeolites were heated from room temperature to 823 K under helium at a rate of 1 K min^{-1} and maintained at this temperature for 6 h. For pre-treatments, 0.5 g catalysts were subjected to a helium flow of 30 ml min^{-1}.

Samples were characterized by elemental analysis, adsorption of N_2 at 77 K, temperature-programmed desorption of O_2 (O_2-TPD), diffuse reflectance infrared Fourier transform spectroscopy (DRIFTS), Raman spectroscopy and XPS.

Adsorption and desorption curves of N_2 at 77 K were obtained with a Micromeritics ASAP 2000 apparatus after degassing the samples at 423 K for 12 h under vacuum. This permitted determination of the surface area and the pore volume of the samples. Micropore measurements performed using the same device were carried out at low N_2 pressures using the Dubinin–Raduskevitch and Horvath–Kawazove formalisms.

The TPD measurements with O_2 were carried out in the same fixed-bed quartz microreactor as that used for the catalytic testing. Four hundred milligrams of the sample were heated from room temperature to 773 K at a rate of 1 K min^{-1} in a diluted flow of O_2 (40%O_2 in He at 27 ml min^{-1}) and kept at 773 K for 8 h. After cooling under an O_2 flow to room temperature, the sample was purged with He (15 ml min^{-1}) for 3 h. The temperature was then increased at a rate of 5 K min^{-1} up to 773 K under the same He flow. The O_2 desorbed was analyzed by a Balzers Quadrupole QMG 311 mass spectrometer.

DRIFTS spectra were recorded by using a controlled-temperature-and-environment diffuse reflectance DRIFTS chamber (Spectra-Tech 0030-103) with ZnSe windows in a Brucker IFS88 infrared spectrometer with KBr optics and using a DTGS detector. The samples were placed inside the chamber without packing or dilution. Before NO adsorption,

Table 1
Chemical composition and surface area of the investigated catalysts

MFI-Sample	Chemical composition				Exchanged Cu (%)	Langmuir surface area ($m^2\,g^{-1}$)	Pore volume ($cm^3\,g^{-1}$)
	Al (wt.%)	Si (wt.%)	Zr (wt.%)	Cu (wt.%)			
Z-0-240	0.33	9.95	0	3.72	240	432	0.16
Z-0.02-241	0.33	10.26	0.02	3.74	241	431	0.15
Z-0-220	0.32	9.91	0	3.31	220	435	0.16
Z-0.21-220	0.31	9.58	0.21	3.20	220	430	0.16
Z-0.32-197	0.30	9.23	0.32	2.77	197	435	0.16
Z-0.49-167	0.33	10.11	0.49	2.59	167	431	0.16
Z-0.78-145	0.32	9.71	0.78	2.18	145	436	0.16
Z-1.94-85	0.33	9.06	1.94	1.24	85	434	0.16

the samples were activated for 1 h at 773 K under 30 ml min^{-1} of He flow. They were subsequently cooled at room temperature in He and the flow rate was switched to 30 ml min^{-1} of 5%NO–He flow. After that, the temperature was increased, and a DRIFTS spectrum was recorded each 100 K after 30 min of stabilization. The spectra were collected for 200 scans at a 4 cm^{-1}resolution. The Raman spectra were recorded on a Dilor–Jobin Yvon-SPEX spectrometer equipped with an optical multichannel analyzer. The Raman spectra were excited with the 488 nm line of an Ar^+-ion laser. Self-supporting wafers were used. These were prepared from powder samples pre-activated for 6 h at 823 K.

The XPS spectra were recorded using an SSI X probe FISONS spectrometer (SSX -100/206) with monochromated AlKα radiation. The spectrometer energy scale was calibrated using the Au $4f_{7/2}$ peak (binding energy 84.0 eV). The samples were moderately heated by a quartz lamp in the introduction chamber of the spectrometer to promote degassing, thus improving the vacuum in the analysis chamber. For the calculation of the binding energies, the C1s peak of the C–(C,H) component at 284.8 eV was used as an internal standard. The composite peaks were decomposed by a fitting routine included in the ESCA 8,3 D software. The superficial composition of the investigated samples was determined using the same software. It used the bands assigned to Cu_{2p3},Cu_{2p1},Zr_{3d5}, Zr_{3d3}, Al_{2s}, $O_{1s}$and Si_{2p}, respectively.

All samples were tested for the decomposition of NO to N_2 and O_2. The tests were carried out in a continuous flow system with a fixed-bed quartz microreactor containing 0.5 g of catalyst. The reactant gas feed contained 4400 ppm of NO with He as carrier gas. The total flow was 30 ml min^{-1} (W/F = 2 g s ml^{-1}). Each catalyst was tested between 623 and 873 K and the products of the reaction were analyzed with an on-line Balzers Quadrupole QMG 311 spectrometer, scanning the masses from 28 to 46*l* The calibration of the apparatus was done using pure gases (Belgair). The analyses accounted for the cracking of nitrogen oxides in the mass spectrometer. The activity of the catalysts was expressed in terms of NO total conversion and NO conversion to N_2.

3. Results

3.1. Implantation of Cu in the zeolite

Data presented in Table 1 shows that starting from the same content of copper in the solution and from the same liquid–solid ratio, the degree of copper exchange is different. Diagram 1 illustrates

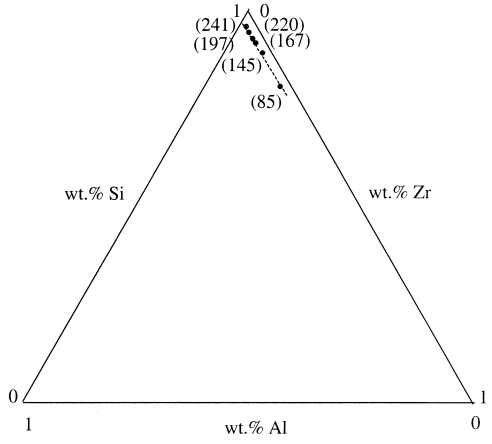

the relation between the chemical composition of the zeolites and the 'exchanged' copper. In this diagram, the chemical composition was normalized considering only three components: Si, Zr and Al. The increase in the content of Zr in the zeolite results in a decrease in the Cu loading. It is noteworthy that this behavior occurs for samples having nearly the same content of aluminum, namely for nearly the same content of exchangeable sites and for almost identical (Si + Zr)/Al ratios. Using a typical ZSM-5 without Zr, the amount of Cu in the solution corresponds to a Cu exchange of ca. 240%, a value which is very close to that obtained using a zeolite containing ca. 0.02 wt.% Zr.

3.2. O_2-TPD

Fig. 2 shows the O_2-TPD profiles corresponding to zeolites with different Cu loadings. These curves exhibit a first prominent maximum centered at about 641 K and a second one around 832 K. The position of these maxima does not depend on the copper content or on the chemical composition of the zeolites, but the areas of the peaks are in direct dependence. The peak located above 641 K corresponds to a collective property of copper and the zeolite and results from the formation of species containing extra-lattice oxygen (ELO) [16,17]. The additional release centered around 832 K results solely from the contribution of isolated Cu species. Table 2 gives the area of these peaks normalized as an O atom-to-metal atom ratio.

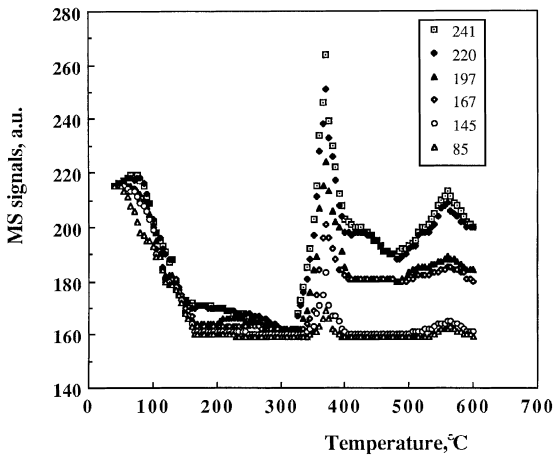

Fig. 2. O_2-TPD profiles of the investigated Cu-ZSM-5 zeolites.

Table 2
Amount of O_2 released from the catalysts studied in O_2-TPD

Cu- Zeolite	O-to-metal atom ratio	
	from the peak centered at 641 K	from the peak centered at 832 K
241	0.12	0.019
220	0.12	0.014
197	0.10	0.015
167	0.07	0.011
145	0.05	0.015
85	0.03	0.015

The number of oxygen atoms assigned to be released from the species containing extra-lattice oxygen decreases with the decrease of the exchanged Cu. On the contrary, the number of oxygen atoms corresponding to the peak centered around 832 K does not depend on the copper exchanged.

Summarizing these results, one can notice that the monitoring of the oxygen released during TPD is mainly sensitive to extra-lattice oxygen species.

3.3. DRIFTS

Fig. 3 shows DRIFTS spectra of zeolites after activation in situ in He at 773 K for 1 h. All the spectra have a similar structure. They contain bands due to the zeolite framework (580, 620, 1200–1370 cm^{-1}), aluminosilicate lattice (800, 1030–1070 cm^{-1}) and ELO (960–970 cm^{-1}). Besides these, another band near 690 cm^{-1} has also been detected. This band could be assigned to the ν_4 stretching vibrations modes of the Cu–O bond [18]. The increase of the Cu content shows some parallel with an increase of the intensity of the band assigned to ELO species and a decrease of the intensity of the band located around 690 cm^{-1}, which is assigned to isolated Cu oxide species. The bands corresponding to ELO species exhibit an observable intensity starting from a Cu content corresponding to a 145% exchange. One also should note that, due to the presence of Zr in the zeolite framework, the structure of the OH bands is different from those corresponding to pure silica–alumina ZSM-5. Three different OH groups located at 3722, 3680, and 3594 cm^{-1} can be observed.

The DRIFTS spectra collected on zeolites with different Cu contents in the presence of NO and for

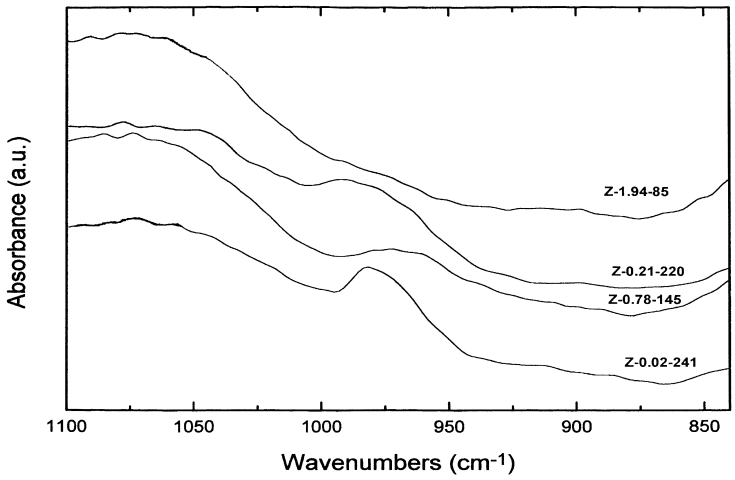

Fig. 3. DRIFTS spectra of the in situ He activated Cu-ZSM-5 zeolites.

various temperatures indicated a different interaction. Fig. 4, as indicated in the figures, corresponds to a subtraction of the spectra collected at successive temperatures. These subtractions were made after a background in He was acquired at each temperature and these backgrounds were used to correct the spectra recorded at each temperature. This allows to follow the evolution of the various chemisorbed species during the investigated steps. In the spectra recorded at room temperature, the subtraction indicates bands located at 1889–1904 cm^{-1}(assigned to $\nu_{(NO)\delta+}$ frequencies), 1854–1856 cm^{-1}(assigned to $\nu_{(N_2O_3)\delta+}$ frequencies), 1673–1700 cm^{-1}(assigned to $\nu_{(NO_2)_2\delta+}$ frequencies), and lower than 1604 cm^{-1}(assigned to nitrate–nitrite species) [19–21]. One should note that, in the conditions of continuous NO–He mixture flow, no bands assigned to gem-dinitrosyl species were detectable. The increase of the contact time to 12 h (Fig. 4(c)) made that the bands assigned to nitrate-nitrite species became more distinct, indicating even at this temperature a slow decomposition process that is in total agreement with numerous papers on this subject [22,23]. The increase of the temperature to 773 K causes a continuous decrease of the bands located at ca. 1894, 1856 and 1673–1700 cm^{-1}, indicating that these species are actually involved in the reaction pathway, as we had indicated previously [21]. One should also remark that both the band assigned to ELO and the one assigned to isolated Cu species diminish with the increase of the temperature in the NO atmosphere. Also, the position of the ELO band changes with the temperature to lower wave numbers, namely to the positions corresponding to Cu^{++} species [24]. Another modification in the spectra recorded in the presence of NO at different temperatures occurred in the region of OH groups. The increase in temperature leads to the formation of new bands (at 3726 cm^{-1} at 373 K, and at 3726, 3693 and 3610 cm^{-1}at higher temperatures). Simultaneously, the bands in the 3600–3400 cm^{-1}range disappear, indicating that the presence of NO is responsible for these changes.

3.4. Raman spectra

Raman spectra recorded for the fresh catalysts (Fig. 5) showed, in addition to typical bands of ZSM-5 lattice, additional bands at 660 and at 635 cm^{-1} which correspond to ν_4 and ν_{12} stretching vibrations modes of Cu–O bonds [18]. A similar band was not evidenced in the case of 240 and 220% Cu exchanged pure ZSM-5. These data could suggest that in the catalysts in which silicon was replaced by zirconium, even for the same concentration of copper as with similar pure ZSM-5 catalysts, an agglomeration of copper takes place. Raman spectra recorded after NO decomposition tests do not contain this band. According to the arguments presented in Section 1, we interpret this as indicating a redispersion of copper (Fig. 6).

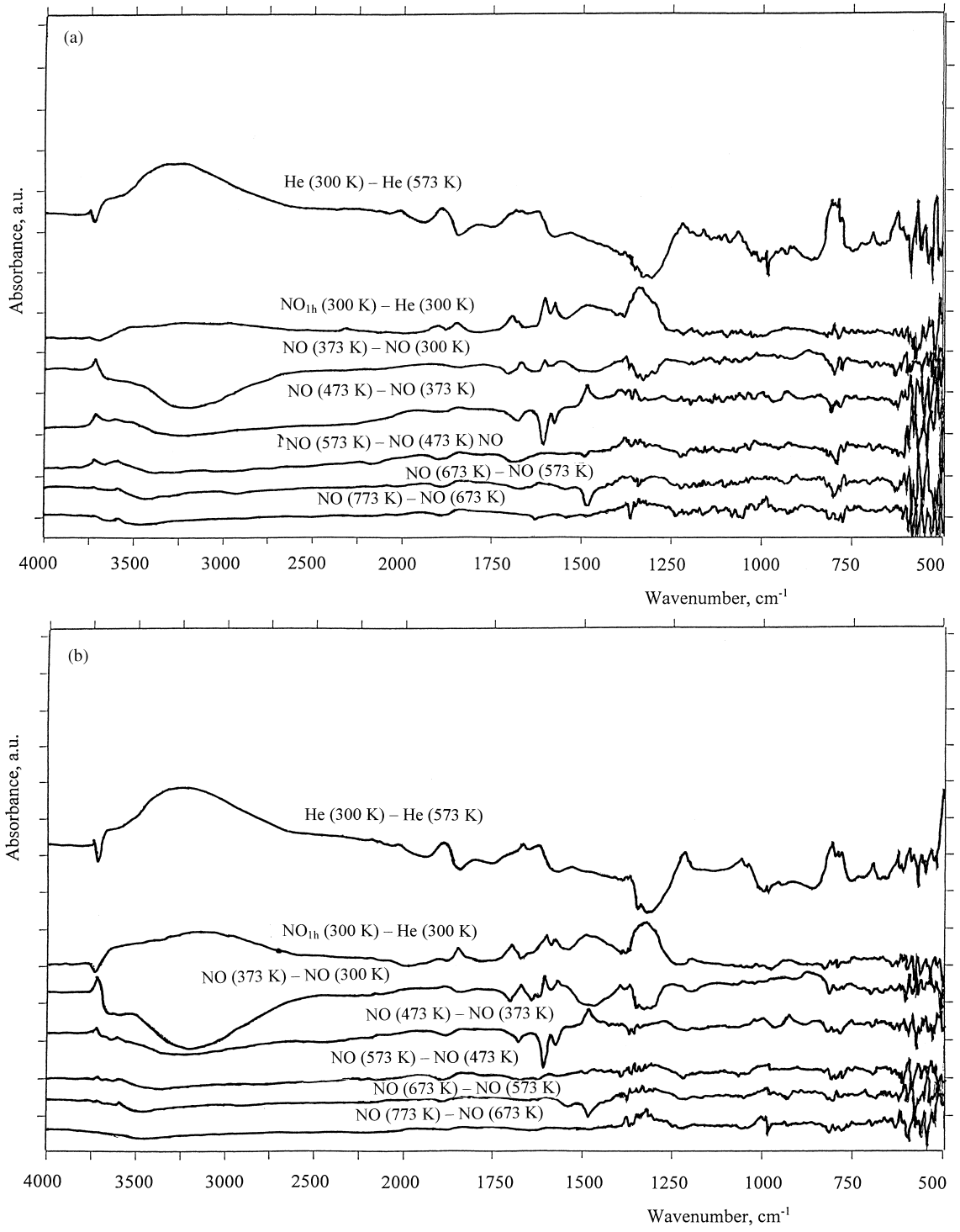

Fig. 4. NO-DRIFTS subtracted spectra of the spectra collected at different temperatures. (a) (Z-0.21–220); (b) (Z-0.32–197); and (c) (Z-0.78–145).

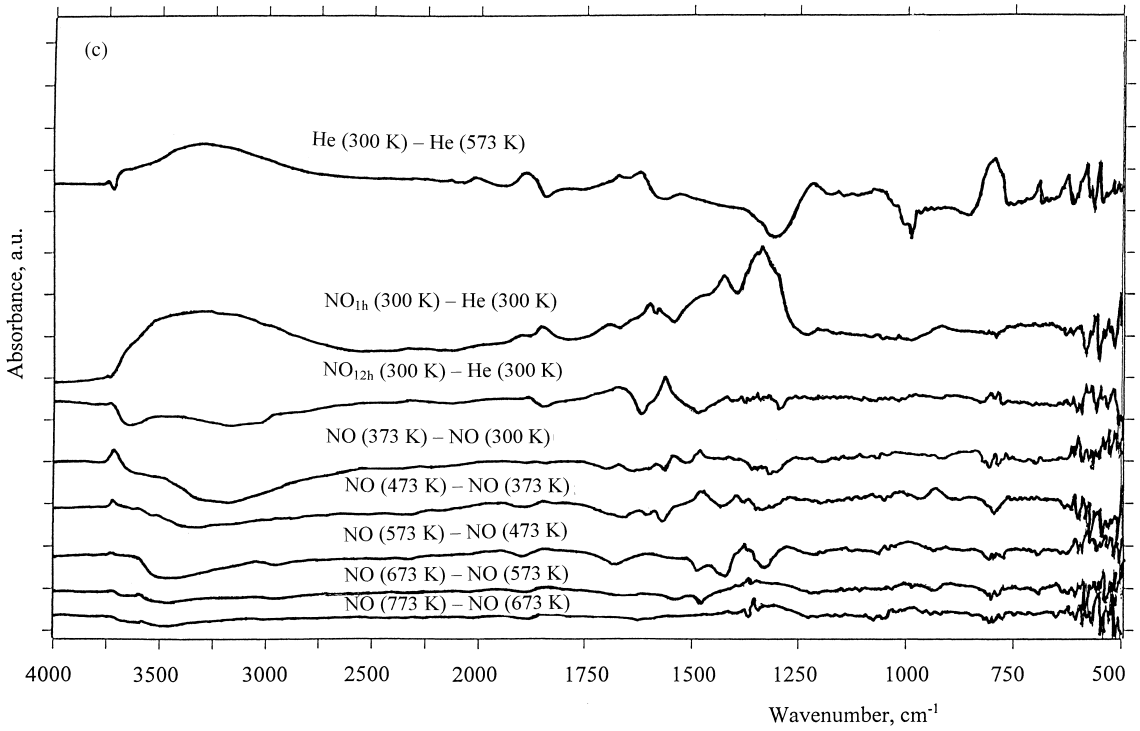

Fig. 4. (*Continued*).

3.5. XPS spectra

Figs. 7 and 8 give the XPS characteristics of the investigated zeolites. No shift in the binding energies of the analyzed elements were determined as a consequence of the modification of the chemical composition of the zeolites. Freshly prepared samples exhibit a higher superficial concentration of Cu compared with the results obtained from chemical analysis (Fig. 7). The same Fig. 7 shows that exposing the samples for 6 h to NO at 823 K leads to a diminution of the Cu signal. All samples show a lower Cu/Si ratio after catalytic tests relative to the data from the elemental analysis results. This is also interpreted as corresponding to a migration of Cu inside the zeolite channels and in such conditions, except for the sample with 85% exchange, the Cu/Si ratio becomes slightly lower than that determined from chemical analysis. Another piece of information obtained from XPS analysis concerns the Cu(I)-to-Cu(II) ratio [25]. In both, the fresh and tested catalysts there is a tendency to a decrease of this ratio with the decrease of the Cu loading, which is in a perfect concordance with DRIFTS and Raman data (Fig. 8). The analysis of the catalysts before, and after, the catalytic tests give comparable results indicating that most of the Cu remains in a (II)-oxidized state. An exception is the (241) catalyst for which, similarly to the use of Cu exchanged pure ZSM-5 zeolites, the XPS Cu(I)-to-Cu(II) ratio after the catalytic tests still indicates about 33% Cu in Cu(I) state.

3.6. Catalytic tests

Figs. 9 and 10 show the catalytic performances of the investigated catalysts. Data presented in these figures were recorded after 3 h of reaction, namely when the reaction reached stationarity. Data obtained on Cu-zeolites containing Zr with given (Si + Zr)-to-Al ratios were compared with those exhibited by 240 and 220% Cu exchanged pure ZSM-5 with a corresponding Si-to-Al ratio. NO conversions to N_2 obtained on Cu-ZSM-5 zeolites in which zirconium replaced

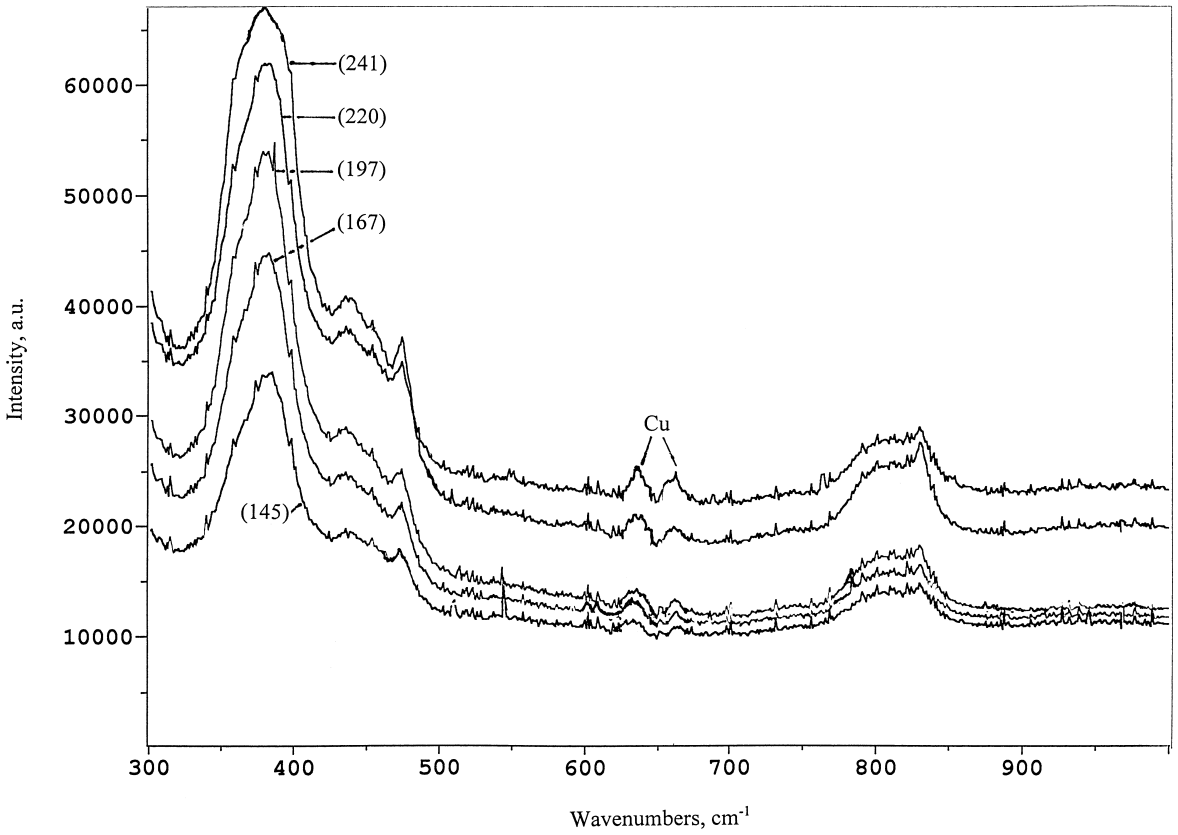

Fig. 5. Raman spectra of the fresh catalysts.

Si were below 40%, which is about 30% lower than those recorded on Cu-exchanged pure zeolites. The total conversion of NO was also smaller than that on the Cu-pure ZSM-5 while the conversion of NO to NO_2 was more important on Cu-implanted in ZSM-5 containing Zr. However, a small amount of Zr, such as 0.02 wt.%, has no influence upon the catalytic behavior of this catalyst.

Differences in behavior as a function of the degree of Cu exchange were also observed. The increase of the copper content up to an exchange value corresponding to 197% has no significant influence on the catalytic behavior of these catalysts. But, an additional increase of the copper loading above this value causes an increase both, in the total conversion and in the conversion to N_2.

One should notice that the very low O_2-to-N_2 ratios on almost all the investigated ranges of copper concentration (Fig. 9) correspond to an important release of NO_2, which actually contains the silent oxygen (Fig. 10).

Concerning the effect of the temperature, we observed the typical behavior for the Cu-zeolite catalysts. The conversion increased from 623 to 823 K, where a maximum was determined for all the catalysts and after that, namely between 823 and 873 K, a decrease occurred.

4. Discussion

The modification of the Zr/Al ratio in the investigated zeolites influences the copper loading. This behavior occurred in spite of an identical copper content in the exchange solution and, what is more important, for nearly the same content of Al in the zeolites,

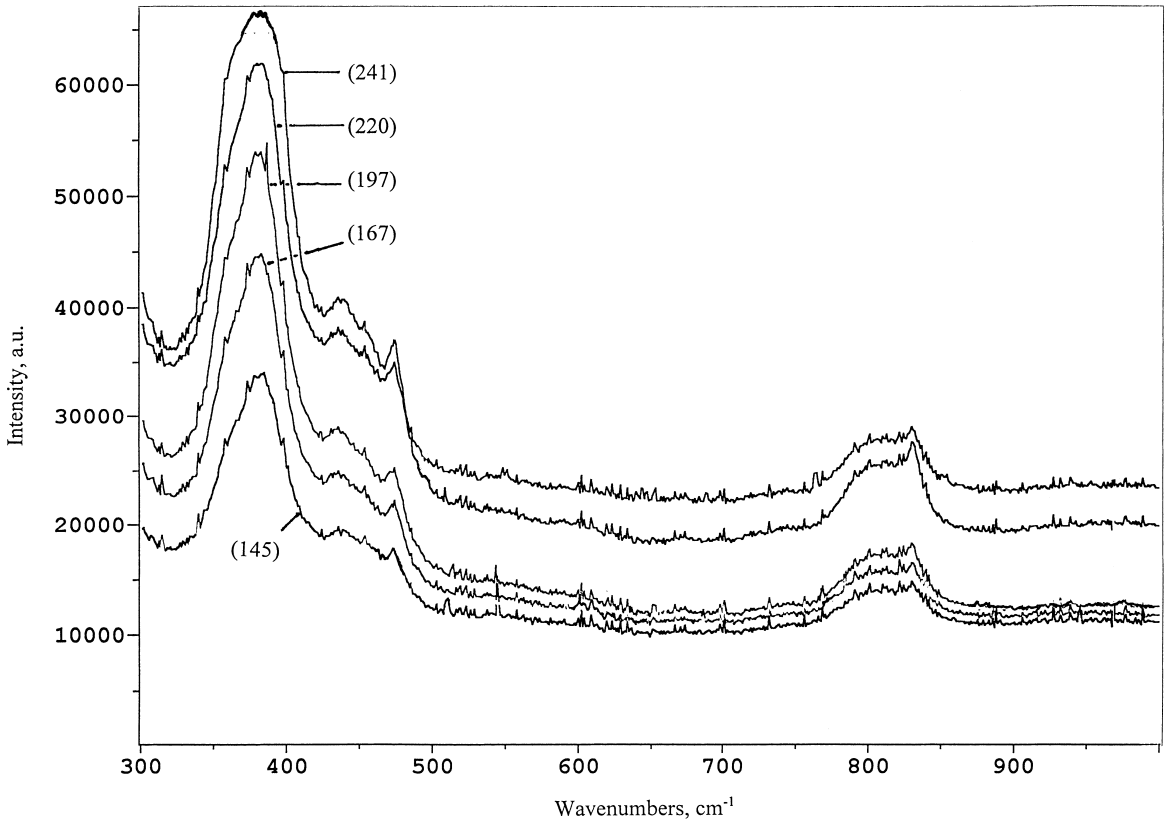

Fig. 6. Raman spectra of the tested catalysts.

namely for nearly the same content of exchangeable sites. Therefore, one can interpret the observed behavior more as a modification of the superficial properties of the zeolites than as an electronic effect of Zr upon the properties of the lattice Al. It seems that the effect of Zr is only to modify the properties of the OH function. This becomes more basic. Actually, the structure of the OH bands determined from DRIFTS for Zr containing zeolites is totally different from those corresponding to pure ZSM-5. Neither XRD nor textural characterization give us any argument in favor of a zeolite lattice damage associated with the presence of Zr. However, we cannot totally exclude the presence of some extra-lattice zirconium species. The modification of the Cu content with the chemical composition of the zeolites cannot be due to the presence of these species because the differences in this content are too high (from 240 to 85% Cu exchange) compared to the possible maximum content of Zr.

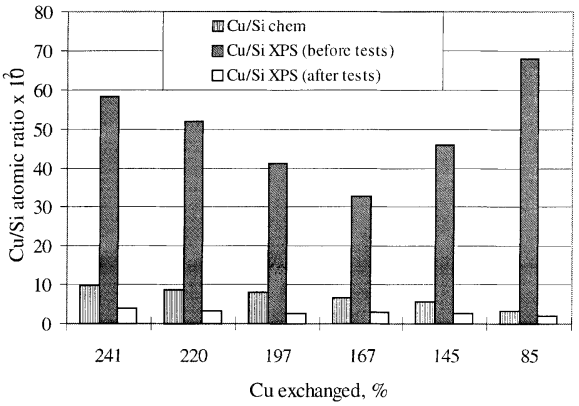

Fig. 7. XPS Cu/Si ratio compared to chemical Cu/Si ratio for the investigated catalysts.

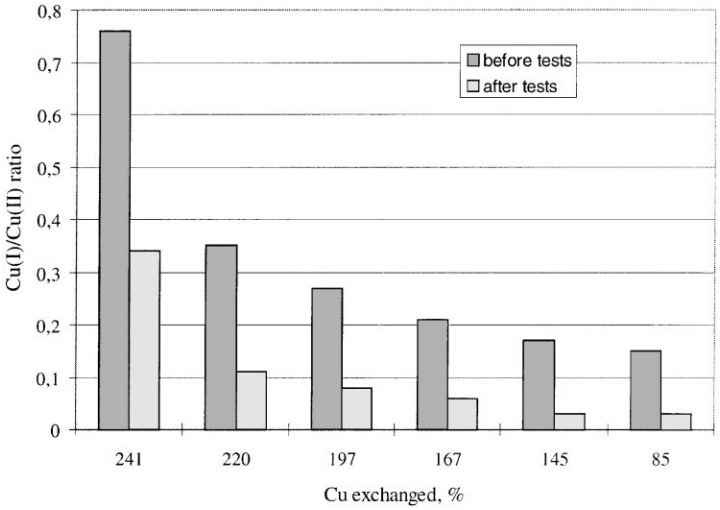

Fig. 8. XPS Cu(I)/Cu(II) ratio for the investigated catalysts.

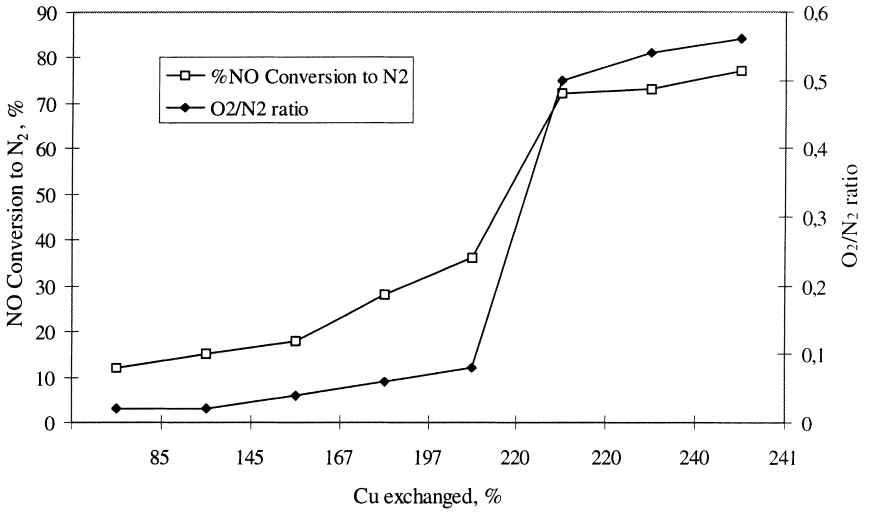

Fig. 9. NO conversion to N_2, and O_2/N_2 ratio for Cu-ZSM-5 zeolites containing Zr compared to Cu-pure ZSM-5. 0.5 g catalyst, flow rate: 30 ml min^{-1}, 823 K, after 3 h.

In a previous paper, we suggested [21], in agreement with other data published in the literature [26], that to achieve an over-exchange, a second Cu atom should be bonded onto the silanol species leading to asymmetric diatomic Cu(II)–O–Cu(I) clusters. This hypothesis was later confirmed by Sayle et al. [27] based on molecular dynamics and computer-aided design calculae of these structures. Using such an assumption one can suppose that the increase of the Zr content should lead to a decrease of the dimer species population. Indeed, the DRIFTS spectra recorded for the in situ He-activated samples indicated that a decrease of the ELO species occurs when the Zr content increases and, as a consequence, the total Cu loading decreases. Another piece of information resulting from the analysis of the DRIFTS spectra concerns the

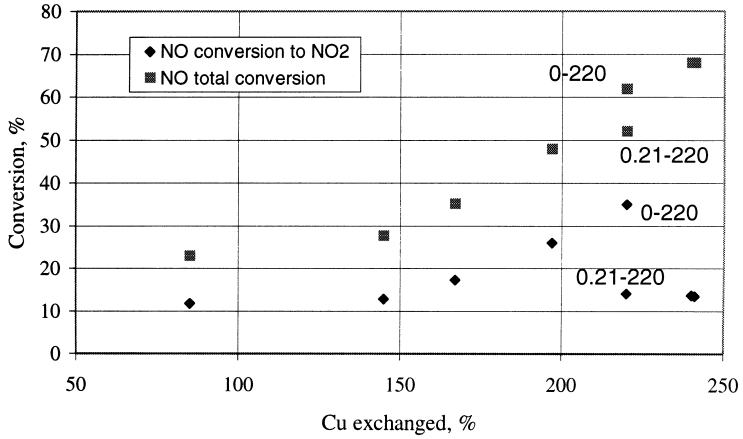

Fig. 10. NO conversion to NO_2, and NO total conversion for Cu-ZSM-5 zeolites containing Zr as compared with Cu-pure ZSM-5. 0.5 g catalyst, flow rate: 30 ml min^{-1}, 823 K, after 3 h.

isolated Cu-oxide. The spectra recorded for different Zr-containing zeolites (Fig. 3) show that the band assigned to these species varies in a direction opposite to that of the ELO species, namely the increase of the Zr content made the presence of these species more evident. This observation is also in perfect concordance with the Raman spectra recorded for the fresh catalysts, which indicated the presence of the same species (Fig. 5). This data allows us to conclude that an increased Zr content leads to a diminution of the ELO species, but to an increase of the isolated copper oxide aggregates. Parallel results were obtained from O_2-TPD analysis. Compared with those determined by chemical analysis, higher copper superficial concentrations were also determined from the XPS Cu-to-Si ratios.

An oxidizing atmosphere, like that generated by the presence of NO, leads to effects which are interpreted as a migration of Cu inside the zeolite channels and/or a redispersion of the Cu containing species. Several findings support this conclusion. The first ones result from in situ NO DRIFTS analysis which showed a decrease of the ELO band intensity with the increase of the temperature, and also a decrease of the band assigned to isolated Cu species, a conclusion which is very interesting. Other evidence was given by Raman spectra, which showed no more Cu components after the catalysts were tested for NO decomposition and by XPS which indicated an important decrease of the Cu-to-Si ratio for the tested catalysts in comparison to the fresh ones.

These copper species, however, migrate to inactive positions. A decrease of the conversion with the increase of the reaction time was observed. After 3 h, the reactions are stationary. Careful analysis of the numerous data published on this reaction shows that ELO species can be easily destroyed during the reaction. But it seems almost impossible, at least for the known zeolites, to reform these species during the reaction. It is even more difficult to create such species starting from copper in the form of oxide.

Summarizing, the reaction data indicated that the conversions were rather low and also corresponded to the low O_2-to-N_2 ratio in the product, an effect which led to the production of a high amount of NO_2.

Our results also shed light on the reaction mechanism. In situ NO DRIFTS analysis showed that part of the reaction occurs via a pathway we have recently proposed [21]. $(NO)^{\delta+}$ species are directly involved in the generation of the active intermediates and successive subtraction of the spectra at different temperatures brings arguments in this sense. The presence of the $(N_2O_3)^{\delta+}$ as well as the $(NO_2)_2{}^{\delta+}$ species leads us to suggest that they are also involved as in the same reaction pathway. We have no evidence to the presence of gem-dinotrosyl species at these temperatures and NO concentrations, but only that of the dimer $(NO_2)_2{}^{\delta+}$

ones. The O_2-to-N_2 ratio we have determined makes us speculate that the reaction also occurs following the scheme proposed by Shelef in which the silent oxygen gets incorporated in the released NO_2 [28].

5. Conclusions

The partial replacement of Si atoms with Zr leads to ZSM-5 materials which, when loaded with Cu, are less effective for NO decomposition than pure ZSM-5. This behavior results from a modification of the superficial properties of the zeolite, which implies that only part of the copper could generate ELO species, while the other one consists of copper oxide agglomerates. Under such conditions these catalysts exhibit a low NO decomposition activity.

Referring to the conclusions of Centi and Perathoner mentioned in Section 1, our results here show that replacing Si by Zr exerts a negative effect.

Acknowledgements

Dr. M.A. Centeno thanks the European Union for a Training and Mobility of Researchers (TMR) postdoctoral grant. We acknowledge the FNRS (Belgium) for financial support.

References

[1] M. Iwamoto, H. Furukawa, Y. Mine, F. Uemura, S. Mikuriya, S. Kagawa, J. Chem. Soc. Chem. Commun. 16 (1986) 1272.
[2] M. Iwamoto, H. Furukawa, S. Kagawa, in: M. Misono, Y. Moro-oka, S. Kimura (Eds.), Future Opportunities in Catalytic and Separation Technology Stud. Surf. Sci. Catal., vol. 54, Elsevier Sci., Amsterdam, 1990, 121.
[3] M. Iwamoto, H. Furukawa, S. Kagawa, in: L. Guczi, F. Solymosi, P. Tetenyi (Eds.), New Frontiers in Catalysis, Proc. 10th Int.Congr.Catal., Budapest 1992, Akademiai Kiado, Budapest, 1993, 1285 pp.
[4] M. Iwamoto, H. Furukawa, S. Kagawa, in: Y. Murakami, A. Iijima, J.W. Ward (Eds.), New Developments in Zeolite Science and Technology, Stud. Surf. Sci. Catal., vol. 28, Elsevier Sci., Amsterdam, 1986, 943 pp.
[5] Y. Li, W.K. Hall, J. Phys. Chem. 94(16) (1990) 6145.
[6] G. Moretti, Catal. Lett. 23 (1994) 135.
[7] V. I. Pârvulescu, P. Oelker, P. Grange, B. Delmon, in A. Andreev, L. Petrov, Ch. Bonev, K. Kadinov, I. Mitov (Eds.), Proceedings of the 8th International Symposium on Heterogeneous Catalysis, Varna, 1996, 1996, 353 pp.
[8] G. Centi, S. Perathoner, Appl. Catal. A: Gen. 132 (1995) 179.
[9] B. Wichterlova, Z. Sobalik, J. Dedecek, A. Vondrova, K. Klier, J. Catal. 169 (1997) 194.
[10] J. Dedecek, B. Wichterlova, J. Phys. Chem. 98 (1994) 5721.
[11] Z. Sobalik, J. Dedecek, I. Ikonnikov, B. Wichterlova, Microporous Mat. 21 (1998) 525.
[12] H. Robson, Microporous Mat. 22 (1998) 551.
[13] H. van Koningsveld, H. van Bekkum, J.C. Jansen, Acta Cryst. B 43 (1987) 127.
[14] H. van Koningsveld, J.C. Jansen, H. van Bekkum, Zeolites 10 (1990) 235.
[15] M. Iwamoto, H. Yahiro, Y. Mine, S. Kagawa, Chem. Lett. 2 (1989) 213.
[16] Y. Li, J.N. Armor, Appl. Catal. 76 (1991) L1.
[17] M. Iwamoto, H. Yahiro, K. Tanda, in: T. Inui (Ed.), Successful Design of Catalysts, Stud. Surf. Sci. Catal., vol. 46, Elsevier Sci. Amsterdam, 1989, 219 pp.
[18] K. Nakamoto, Infrared and Raman Spectra of Inorganic and Coordination Compounds, 4th ed., Wiley-Interscience, New York, 1976.
[19] A.W. Aylor, S.C. Larsen, J.A. Reimer, A.T. Bell, J. Catal. 157 (1995) 592.
[20] K. Hadjiivanov, D. Klissurski, G. Ramis, G. Busca, Appl. Catal. B: Environm. 7 (1996) 251.
[21] V.I. Pârvulescu, P. Grange, B. Delmon, J. Phys. Chem. B 101 (1997) 6933.
[22] M. Iwamoto, H. Yahiro, N. Mizuno, W.-X. Zhang, Y. Mine, H. Furukawa, S. Kagawa, J. Phys. Chem. 96 (1992) 9360.
[23] E. Giamello, D. Murphy, G. Magnacca, C. Morterra, Y. Shioya, T. Nomura, M. Anpo, J. Catal. 136 (1992) 510.
[24] J. Sarkany, W.M.H. Sachtler, Zeolites 14 (1994) 7.
[25] V.I. Pârvulescu, P. Oelker, P. Grange, B. Delmon, Appl. Catal. B: Environm. 16 (1998) 1.
[26] D.J. Parrillo, J.P. Fortney, R.J. Gorte, R.W. McCabe, J. Catal. 142 (1993) 708.
[27] D.C. Sayle, C.R.A. Catlow, J.D. Gale, M.A. Perrin, P. Nortier, J. Mater. Chem. 7 (1997) 1635.
[28] M. Shelef, Catal. Lett. 15 (1992) 305.